Phase-conjugate four-wave mixing with partially coherent laser fields

Binh Do
Department of Physics and School of Electrical and Computer Engineering, Purdue University, West Lafayette, Indiana 47907

Jongwhan Cha and D. S. Elliott
School of Electrical and Computer Engineering, Purdue University, West Lafayette, Indiana 47907

S. J. Smith
JILA, University of Colorado and the National Institute for Standards and Technology, Boulder, Colorado 80309
(Received 13 October 1998)

We present results of our experimental investigations of phase-conjugate four-wave mixing in a nearly Doppler-free, collisionless, two-level quantum system with a partially coherent non-Markovian laser field. The two components of the laser field—an intense pump and a weak, time-delayed probe—are derived from a single narrow-band cw laser source on which phase and frequency fluctuations conforming to the phase diffusion model are superimposed. We carry out these measurements using the D_2 transition in an optically pumped diffuse beam of atomic sodium. We vary the pump intensity, laser bandwidth, and temporal delay between the pump and probe, and measure the peak signal strength, the bandwidth, and the asymmetry of the four-wave-mixing spectrum. For comparison with our experimental results of the peak signal strength, we also analyze the same interaction numerically, through direct integration of the optical Bloch equations. The numerical results are in good agreement with the measurements. [S1050-2947(99)00307-8]

PACS number(s): 42.50.Gy, 32.80.−t, 42.65.Hw

I. INTRODUCTION

Coherent interactions between laser fields and atomic systems can be used to create coherent superposition states with unique properties. The coherence transferred to the atom by a laser field is manifested in a variety of optical phenomena and coherent atomic systems, including, for example, population-trapped (or dark) states, optical gain without a population inversion, electromagnetically induced transparency, and photon echoes. Laser sources do not generally produce perfectly coherent fields, however, and it becomes of interest to study how the partial coherence of a laser field influences these inherently coherent atomic states. In this paper, we report our experimental measurements of phase-conjugate four-wave mixing in a collimated, collisionless atomic beam of two-level sodium atoms with a cw laser field whose frequency and phase are undergoing random fluctuations.

The measurements which we discuss are directly related to a series of investigations which have been carried out over the past decade and a half in which broadband nanosecond-duration pulses have been used to drive various four-wave mixing interactions to measure subpicosecond relaxations in media. This effect was observed by Beach and co-workers [1] and by Asaka *et al.* [2]. In each case, the investigators used a beam splitter to derive two broadband optical pulses from a single laser source, and directed these two pulses into a nonlinear medium (sodium vapor in Ref. [1] and Nd^{3+}-doped silicate glass in Ref. [2]). A schematic representation of their experimental geometry is shown in Fig. 1(a). They measured the energy of the output pulse generated via a four-wave-mixing interaction propagating in the direction $2\vec{k}_2-\vec{k}_1$, where the wave vectors for the two input pulses are defined as $\vec{k}_1$ and $\vec{k}_2$, as a function of the delay time, τ_d, between the arrival of the two input pulses. A remarkable result of both of these measurements was that picosecond transient responses of the nonlinear media could be observed using nanosecond duration lasers.

Morita and Yajima [3] presented a detailed analysis of this four-wave-mixing signal, valid in the limit of weak fields, and showed that the temporal resolution was limited by the correlation time of the optical field, τ_c. For broadband pulses, the correlation time is in general much shorter than the pulse duration τ_p. This result at first seems completely contrary to experience and intuition.

The qualitative explanation for the mechanism for these

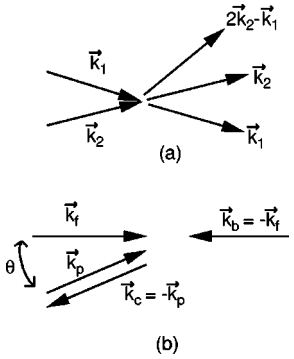

FIG. 1. Wave-vector diagram for four-wave mixing interactions in the (a) forward-beam geometry and (b) phase-conjugate geometry. In (a), input beams in the directions $\vec{k}_1$ and $\vec{k}_2$ produce a new beam in the direction $2\vec{k}_2-\vec{k}_1$. In (b), counterpropagating pump beams ($\vec{k}_f$ and $\vec{k}_b$) and a probe beam ($\vec{k}_p$) interact with the nonlinear medium to produce the phase-conjugate beam ($\vec{k}_c$).

 ©1999 The American Physical Society

four-wave mixing (FWM) results is perhaps best given in terms of the coherent optical effect known as stimulated photon echoes. (Ye and Shen [4] formalized the relationship between photon echoes and the more general process of four-wave mixing.) Stimulated photon echoes are observed when a sequence of three short, coherent pulses is incident upon a medium. The coherent response of the system generates a temporally delayed optical output pulse. One can model the FWM interaction as the echo signal which would result when each input pulse consists of $N=\tau_p/\tau_c$ coherent subpulses. Each of the subpulses within the pulse is incoherent with respect to all the others. A coherence of the medium set up by the medium's interaction with the ith subpulse of the first pulse can be interrogated by the ith subpulse of the second pulse, but not by the jth subpulse of the second. Delays between the optical pulses on the order of the atomic dephasing time T_2 or longer allow the coherence setup by the first pulse to die away before the mutually coherent subpulse of the second pulse arrives, so that the optical output vanishes. This argument explains the sensitivity of the transient four-wave mixing signal with nanosecond (or longer) broadband input pulses to picosecond delays between the two input pulses, with the temporal resolution of the measurement limited by τ_c.

Time-delayed correlated pulses derived from long-duration incoherent light sources were subsequently used in the measurement of relaxation rates in several systems [5–11]. These include Cresyl fast violet dye in a cellulose film [5], alkali metal-argon mixtures [6], sodium vapor [7], Rhodamine 6G dye in solution [8], dimethylsulfoxide [9], carbon disulfide and nitrobenzene [10], and semiconductor-doped glasses [11]. Dephasing times as short as $T_2=5$ fsec were reported in Ref. [11].

A great deal of effort has gone into understanding these effects when the field intensities approach or exceed the saturation intensity for the transition. The use of time-delayed pulses derived from the same source, the basis of all these experiments, constitutes a nontrivial problem for theoretical analysis, especially at elevated intensities, since the total field is non-Markovian. Field and system correlations become extremely complicated. Physically, we think of each pulse influencing the time evolution of the system, but in a statistically correlated way.

The group of Keller and Le Gouët have carried out a series of theoretical and experimental investigations in which they explore the intensity dependence of four-wave mixing with broadband pulses [12–16]. Most of their work concentrated on the turn-on time of the four-wave mixing signal in the direction $2\vec{k}_2-\vec{k}_1$ as the delay time between the two pulses was varied through zero. In the weak-field limit, they showed [12] that the turn-on time of the FWM signal consisted of two components. The time scale of the fast component is the inverse of the (inhomogeneous) Doppler width of the absorption line, while for the second it is the laser-pulse duration τ_p. For intense fields, they showed that the lifetime of the excitation memory is given approximately by τ_c, the correlation time of the field fluctuations, which can be much shorter than the effective interaction time [16].

There are few theoretical analyses valid for arbitrary intensities of each of the input pulses. Friedberg and Hartmann [17] and Tchénio *et al.* [14] developed a diagrammatic technique for calculating the response of two-level atoms to coherent or incoherent laser fields, suitable for the analysis of time-delayed four-wave mixing. Finkelstein and Berman [18,19] reported calculations of FWM by broadband-correlated pulses. In Ref. [18], the first two pulses were intense and overlapping in time, while the third pulse was weak, delayed (i.e., $\tau_d>\tau_p$), and uncorrelated with the first two pulses. Their work showed that many spatially distinct beams can be created for strong input fields, and that the energy of these various signals can be comparable to one another. The low-order signals can exhibit a peak at $\tau_d=0$ whose width is approximately given by τ_c. They also showed that higher-order signals can exhibit an asymmetric dependence on the delay time. In Ref. [19], the authors considered a case similar to the experiments using two input pulses described above. They showed that in this case the signal generated by the coherent interaction can also exhibit a narrow peak of width τ_c, as long as the Doppler width of the nonlinear system is sufficiently narrow.

Four-wave mixing in the forward-beam geometry in a two-level atomic system by broadband continuous wave (cw) laser fields was studied by Vemuri and co-workers [20,21] by numerically integrating the optical Bloch equations for a two-level atomic system. They considered Gaussian fields (random complex amplitude fluctuations) [20] and phase diffusion fields (random phase–frequency fluctuations) [21]. In all cases they calculated that the FWM signal initially decreases with increasing τ_d. For high intensities and nearly Lorentzian laser spectra, they reported that the FWM signal reaches a local minimum, after which it increases toward a fixed intensity-dependent value. In the case of the phase diffusion model (PDM) field, they observed a slight modulation of the amplitude of the FWM signal as a function of τ_d at the Rabi frequency of the interaction.

Phase-conjugate four-wave mixing (PCFWM), as represented in Fig. 1(b), by incoherent fields has received far less attention over the years. In PCFWM, a forward and a backward pump beam propagate exactly antiparallel to one another, and a weak probe field is incident in a direction making a small angle θ with respect to the forward pump beam. These input fields are all at the same frequency ω_L. The interaction with the nonlinear medium produces a fourth field component, also at the frequency ω_L, which propagates back on the incident probe beam. This field is called the phase-conjugate field, since it can be shown that its wave fronts are exactly reversed from those of the probe field. Examples of PCFWM with broadband fields include single-shot measurements of four-wave mixing spectra in a flame [22], PCFWM with incoherent pulses of near-resonant light in a sodium vapor cell [23], and resonant four-wave mixing in the OH radical in a methane-air flame [24]. Nonresonant four-wave mixing with broadband fields was considered theoretically in Ref. [25].

A related phenomenon of optical absorption and gain of a weak cw PDM probe beam by a two-level atomic system driven by an intense time-shifted cw PDM laser field has also been studied theoretically [26] and experimentally [27], with very close agreement between the two. The gain in this system displayed features similar to those we observe in the present work.

Each of the experimental studies of FWM in the forward geometry [1,2,5–13,15,16] and FWM in the phase-conjugate geometry [22–24] quoted above have been carried out in condensed phase or Doppler-broadened vapor-phase media, using the amplified spontaneous emission of a highly pumped gain cell or a misadjusted mode-locked laser. While there has been good overall agreement between theory and experiment, it is our goal to provide a more stringent test of the theoretical techniques and results by performing a series of experimental measurements under conditions which better isolate the effects we seek to study. In the present report, we discuss our detailed measurements of degenerate phase-conjugate four-wave mixing with partially coherent fields. Our nonlinear medium is an atomic two-level system with negligible collisional effects and minimal Doppler broadening. The laser field for our studies is derived from the cw output of a frequency-stabilized dye laser, onto which we impose random frequency and phase fluctuations. Thus we can control and characterize its statistical properties within the context of the fully quantitative phase diffusion field model. We measure the spectrum of the FWM signal as we tune the frequency of the pump and probe field through the atomic resonance frequency, as a function of the laser bandwidth, the intensity of the pump beam, and the delay time between the pump and probe components. We determine the peak signal strength relative to the FWM signal generated by narrow-band fields, as well as the spectral width and asymmetry of the signal. We discuss our measurements in detail in Sec. II. We present our experimental results in Sec. III. In this section we also present the results of a numerical analysis of the peak signal strength of this interaction. We defer details of this analytical technique to the Appendix. We close with a brief conclusion in Sec. IV.

II. EXPERIMENT

In this section we discuss the experimental techniques we use for measurements of phase-conjugate four-wave mixing. We show the geometry of the interaction in Fig. 1(b). Our primary objectives in setting up the experimental configuration were to define the nonlinear medium as a closed, two-level atomic system in a collision-free environment with minimal Doppler broadening; to assure uniform intensity of the pump beam in the interaction region; and to use a laser field whose phase and frequency fluctuations are well characterized and controllable.

The experimental setup, shown schematically in Fig. 2, is very similar to that which we have previously reported [28], except for additional provisions for superimposing phase and frequency fluctuations prescribed by the phase diffusion model onto the pump and probe laser fields. A comprehensive discussion of this noise simulation methodology was presented in Ref. [29]. For this system, we use voltage noise generated by a commercial shot-noise diode source (which produces Gaussian noise with a relatively flat noise spectrum) to drive a voltage-controlled oscillator, producing a constant amplitude, fluctuating frequency rf signal. We limit the bandwidth of the noise from the noise source to 6 MHz to stay within the optimal operating range of the acousto-optic modulator. We separately impose high-frequency phase

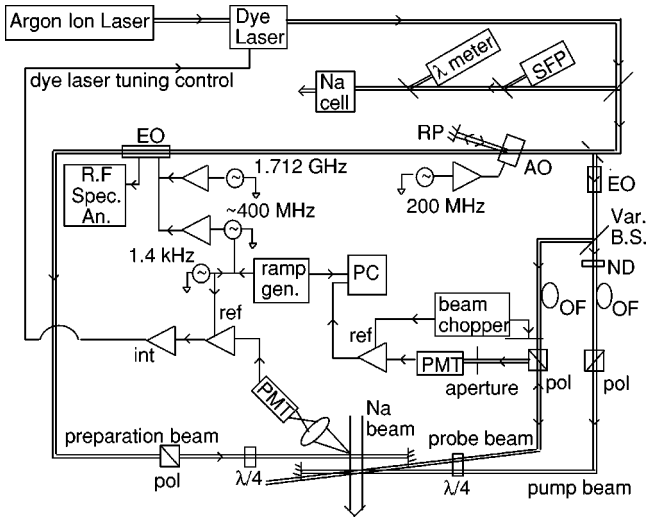

FIG. 2. Schematic diagram for the phase-conjugate four-wave-mixing experiment. Abbreviations in this diagram are used for the scanning Fabry-Perot interferometer (SFP), the acousto-optic modulator (AO), the electro-optic modulator (EO), the roof prism (RP), single-mode optical fibers (OF), photomultipliers (PMT), a personal computer (PC), polarizers (pol), and quarter-wave retarders ($\lambda/4$).

(6–200 MHz) fluctuations onto the laser beam using an electro-optic modulator. The reasons for using a hybrid modulation technique of frequency modulation for low-frequency noise and phase modulation for high-frequency noise lie in the technical advantages offered by each in their respective frequency ranges. These noise spectra are superposed on well-stabilized (bandwidth $\sim$250 kHz) continuous-wave-generated pump and probe beams.

The PDM is characterized by a constant amplitude E_0 but fluctuating frequency $\dot{\phi}(t)=d\phi(t)/dt$,

$$E(t)=E_0\exp\{-i[\omega_L t+\phi(t)]\}. \tag{1}$$

The fluctuating phase $\phi(t)$ is a random Gaussian variable whose dynamics are analogous to those of the position of a particle undergoing Brownian motion. The net result is that, for the spectrum of the Gaussian noise we employ, the frequency fluctuations are exponentially correlated,

$$R_{\dot{\phi}}(\tau)=\langle\dot{\phi}(t)\dot{\phi}(t+\tau)\rangle=b\beta\exp(-\beta|\tau|), \tag{2}$$

where β^{-1} is the correlation time of the fluctuations, and b is the spectral density of the frequency fluctuations. The power spectrum of the frequency fluctuations is Lorentzian in shape, with a 3-dB cutoff frequency of $\beta/2\pi$. In the limit of fast, low-amplitude frequency fluctuations (i.e., $\beta\gg b$), the power spectrum of the optical field is nearly Lorentzian in shape,

$$P_E(\omega)=\frac{E_0^2}{2}\frac{2b}{(\omega-\omega_L)^2+b^2}, \tag{3}$$

with a full width at half maximum (FWHM) of $2b$. The correlation time of this field is $\tau_c=b^{-1}$. We consider only this limit in the present work, in which $\beta/2\pi=100$ MHz and $2b/2\pi$ is 9.0, 14, or 24 MHz.

We chose atomic sodium (specifically, we use the D_2 transition at $\lambda = 589.0$ nm) as our nonlinear medium for this work, and use standard optical pumping techniques [30] to produce a true closed, two-level atomic system consisting of the $3s\,^2S_{1/2}, F=2, m_F=2$ ground state and the $3p\,^2P_{3/2}, F=3, m_F=3$ excited state. The saturation intensity at resonance for this transition is $I^0_{\rm sat} = 6.33 \text{mW cm}^{-2}$, where $I^0_{\rm sat}$ is defined as

$$I^0_{\rm sat} = \frac{\epsilon_0 c \hbar^2 \gamma_{12} \Gamma_0}{2|\mu_{12}|^2}, \tag{4}$$

γ_{12} is the transverse relaxation rate, Γ_0 is the population decay rate, and μ_{12} is the transition dipole moment. The laser beam (labeled the preparation beam in Fig. 2) which drives the sodium into the two-level system also serves to recover the atoms initially in the $F=1$ ground state, helps to collimate the atomic beam, and provides an error signal which we use to control the frequency of the laser. We discuss the complete details of the preparation beam in Ref. [28]. The sodium atomic beam, generated using a single-chamber effusive oven (300°), has a density in the interaction region of 2.7×10^8 atoms per cm^3. The atomic transverse velocity distribution has a width (FWHM) of 300 cm/sec, corresponding to a Doppler width of about 5 MHz.

In the interaction region, we cross the pump and probe fields with the atomic beam at right angles to minimize the Doppler broadening effects. The pump beam and probe beam are collimated, and nearly parallel to one another, crossing at an angle of $\theta \sim 10$ mrad. We vary the delay time τ_d between the pump and probe beams by replacing one of the single-mode optical fibers through which each beam passes with one of a different length. We produce the backward pump beam by reflecting the forward pump beam back on itself after it exits from the vacuum chamber. The round trip time required for the pump beam to travel from the interaction region to the external reflector and back to the interaction region is ~ 2 nsec. The beam radius (defined as the radius at which the intensity drops to e^{-2} of its on-axis intensity) of the pump beam (1.42 mm) is four times larger than that of the probe beam (0.34 mm), assuring that as the beams cross in the interaction region, the intensity of the pump beam is uniform to within 15% where the probe intersects it. At the atomic beam density of our experiments, there are 1.5×10^5 atoms within the volume of the interaction region, as defined by the cross-sectional area of the probe beam and the width of the atomic beam (~ 3 mm).

We measure the weak-field absorption spectrum of the sodium beam in order to monitor the alignment of the laser beams, the alignment of the magnetic dipoles, the collimation of the atomic beam, and the density of the atomic beam. We cancel the Earth's magnetic field to within 10 mG, and impose a field of about 0.5 G along the direction of propagation of the pump field. The width of the absorption spectrum is typically 12.5–14.5 MHz, only slightly larger than the 10-MHz natural linewidth of the transition. The peak absorption of the intensity by the sodium beam is about 12%.

The phase-conjugate beam generated through the nonlinear action of the atoms propagates counter to the direction of the incident probe beam. We use polarization optics to separate the phase-conjugate beam from the probe beam and direct it toward a photomultiplier. The photomultiplier output is amplified in a lock-in amplifier, with the reference input (at ~ 160 Hz) to the lock-in amplifier being generated by the beam chopper of the probe beam. The output of the lock-in amplifier is recorded by a laboratory PC using an external A/D converter, which concurrently records the scan voltage which indirectly tunes the laser frequency [28].

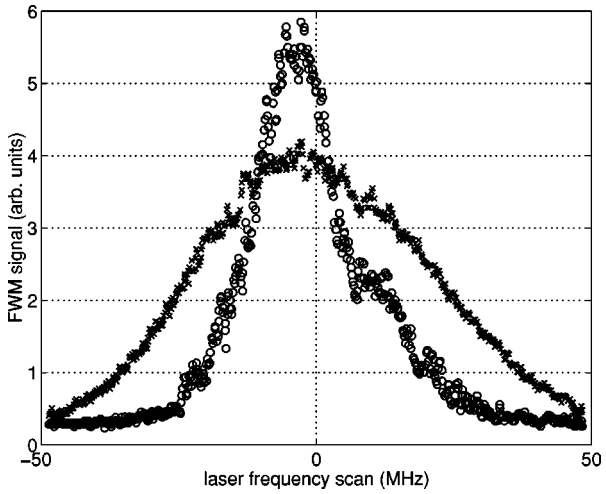

FIG. 3. Typical FWM spectra. The data points shown as circles correspond to the case where the laser noise is turned off, resulting in a laser bandwidth of ~ 250 kHz, while the $\times$'s correspond to a laser bandwidth (FWHM) of 24 MHz at a delay time of -9.9 nsec. The pump beam intensity is 29 mW/cm^2 $= 4.6\ I^0_{\rm sat}$ for both.

For each value of the pump laser power, delay time, and spectral width of the field, we scan the pump and probe frequency together through the resonance frequency of the sodium D_2 transition, and record the power of the phase-conjugate signal as a function of the optical frequency. The intensity of the probe beam is held constant at $0.17\ I^0_{\rm sat}$ (2-μW power). Two typical spectra are shown in Fig. 3. The intensity of the pump beam for these two spectra is 29 mW/cm^2 $= 4.6\ I^0_{\rm sat}$. The data points shown as circles correspond to the case where the laser noise is turned off, while the $\times$'s correspond to a laser bandwidth (FWHM) of 24 MHz and delay time between the pump and probe -9.9 nsec $= -0.31 T_2$. Overall, we measure FWM spectra at five different values of the pump intensity ranging from $0.07\ I^0_{\rm sat}$ to $12\ I^0_{\rm sat}$, and at three different laser bandwidths 9, 14, and 24 MHz. For each measurement, we record four spectra, two with the laser noise on and two with the laser noise off. The FWM spectra with the laser noise on are characterized by a broader width and lower peak value in every case. Each scan is of length 100 MHz, and requires about 100 sec to accumulate.

The spectra often display a dip on the high-frequency side, especially for large pump powers and narrow laser bandwidths. A moderate example of this can be seen in the narrow peak of Fig. 3. We believe this is a result of the pump beam heating the transverse velocity of the atoms, decreasing the number of atoms available to contribute to the four-wave mixing signal [28].

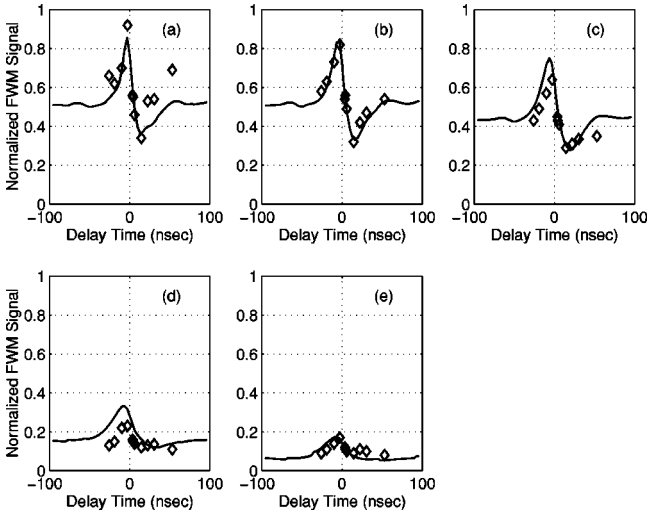

FIG. 4. Normalized FWM signal strength vs the delay time between the pump and probe beams, τ_d, for a laser bandwidth (FWHM) of $b/\pi = 24$ MHz. The experimental measurements are shown as diamonds, while the numerical results are given by the solid lines. The laser intensities $(I/I^0_{\rm sat})$ and Rabi frequencies $(\Omega/2\pi)$ for the five figures are (a) 12 and 24 MHz, (b) 4.6 and 15 MHz, (c) 2.3 and 11 MHz, (d) 0.46 and 4.8 MHz, and (e) 0.185 and 3.0 MHz, respectively.

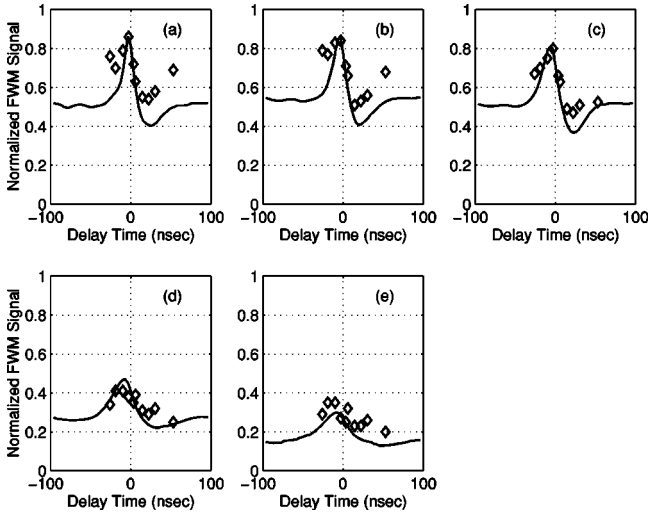

FIG. 5. Normalized FWM signal strength vs the delay time between the pump and probe beams, τ_d, for a laser bandwidth (FWHM) of $b/\pi = 14$ MHz. The experimental measurements are shown as diamonds, while the numerical results are given by the solid lines. The laser intensities $(I/I^0_{\rm sat})$ and Rabi frequencies $(\Omega/2\pi)$ for the five figures are (a) 12 and 24 MHz, (b) 4.6 and 15 MHz, (c) 2.3 and 11 MHz, (d) 0.46 and 4.8 MHz, and (e) 0.185 and 3.0 MHz, respectively.

We have covered the entire range of pump intensities which yield an acceptable signal-to-noise ratio for the phase-conjugate (signal) beam. The most significant source of noise is laser light scattered from the windows of the vacuum system. For pump intensities less than 0.07 $I^0_{\rm sat}$, the signal is detectable, but very weak. For pump intensities greater than 12 $I^0_{\rm sat}$, the signal strength is decreasing due to saturation effects, and we also observe an instability in the signal which makes it difficult to measure the FWM intensity accurately. We do not have an explanation for this instability, but intend to study it in detail in a future work. For our beam density, the maximum phase-conjugate reflectivity for narrow-band fields is $\sim 10^{-4}$, so that our 2-μW probe beam produces a 0.2-nW phase-conjugate beam. The weakest signals we detected were as small as 10 pW. From spectra like those shown in Fig. 3, we determine the peak signal strength, the frequency width of the peak, and the asymmetry of the peak. We will present and discuss these results in Sec. III.

III. RESULTS AND DISCUSSION

In Figs. 4, 5, and 6, we show plots of the peak FWM intensity as a function of τ_d, the delay time between the pump and probe beams. The curves shown in the three figures are given for different laser bandwidths, $b/\pi = 24$, 14, and 9 MHz (FWHM), respectively. The experimental data for five different pump-laser intensities are shown in each figure by the diamond symbols ($\diamond$). In these figures we also present the results of a numerical computation of this interaction, represented by the solid lines. We present essential details of these computations in the Appendix. For laser bandwidths of $b/\pi = 24$ and 14 MHz, the intensities we use are $I/I^0_{\rm sat} = 12$, 4.6, 2.3, 0.46, and 0.185. The corresponding Rabi frequencies $\Omega = [(I/I^0_{\rm sat})\gamma_{12}\Gamma_0]^{1/2}$ at each of these pump intensities are $\Omega/2\pi = 24$, 15, 11, 4.8, and 3.0 MHz, respectively. As a point of reference, the natural linewidth of the D_2 transition in sodium is 10 MHz. For the 9-MHz laser linewidth data shown in Fig. 6, we use the same values for the pump beam intensity except for the lowest intensity, which is 0.07 $I^0_{\rm sat}$, corresponding to a Rabi frequency of 1.9 MHz. There are no adjustable parameters in the experimental or computational results shown in Figs. 4, 5, and 6. All of the

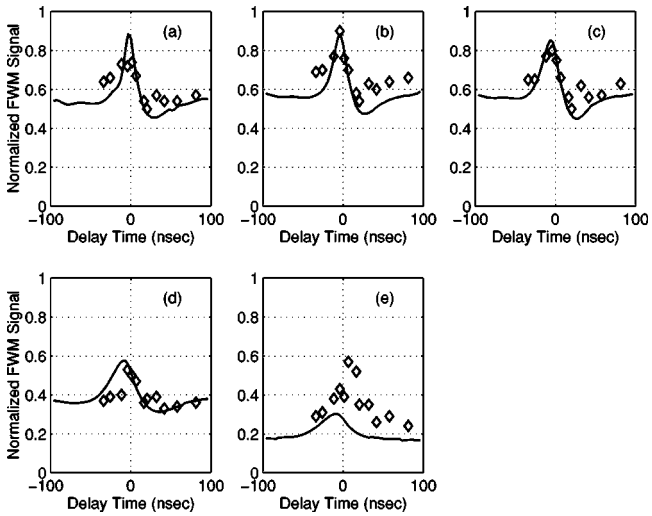

FIG. 6. Normalized FWM signal strength vs the delay time between the pump and probe beams, τ_d, for a laser bandwidth (FWHM) of $b/\pi = 9$ MHz. The experimental measurements are shown as diamonds, while the numerical results are given by the solid lines. The laser intensities $(I/I^0_{\rm sat})$ and Rabi frequencies $(\Omega/2\pi)$ for the five figures are (a) 12 and 24 MHz, (b) 4.6 and 15 MHz, (c) 2.3 and 11 MHz, (d) 0.46 and 4.8 MHz, and (e) 0.07 and 1.9 MHz, respectively.

experimental measurements and the theory are in very good qualitative agreement, and in many cases good quantitative agreement as well. In order to account for any variations in alignment, we report our results as the ratio of the peak height of the FWM spectra with the laser noise turned on to the peak height taken with the narrow-band laser.

In each case, the FWM signal reaches a maximum value when the delay time τ_d is small and negative. As the delay between the pump and probe increases in the positive direction, the FWM signal decreases rapidly, with the slope of this decrease being the greatest for large Ω and large laser bandwidth. Similar behavior was observed in measurements of fluctuation-induced gain in a weak phase-diffusing probe beam interacting with a two-level system driven by a time-delayed correlated phase-diffusing pump beam [26,27], and in numerical calculations of four-wave mixing in a forward-beam geometry [20,21]. We have examined the maximum slope of the unnormalized numerical curves, and find it proportional to Ω^2. For large delay (positive or negative), the pump and probe beams are largely uncorrelated, and the FWM signal approaches a long-delay-time value. The long-delay-time value is ~ 0.5 for large Ω, but drops off significantly for small Ω. In many cases the FWM intensity reaches a minimum before rising to the long-delay-time value, as seen in both the numerical results and in the experimental results. At low pump intensities, there is no local minimum in the figures, as the atomic coherence decreases monotonically to reach the long-delay-time value. The signal strength reaches this value by $\tau_d = 2T_2$, where $T_2 = 32$ nsec, in nearly every case. For delays longer than $2T_2$, the phase of the atomic dipole set up by the pump is uncorrelated with the phase of the probe. The FWM signal for broadband low-intensity fields is very small compared to the narrow-band case, as can be understood in terms of the spectral overlap between the laser spectrum and the atomic absorption line.

Because of the complexity of the statistical properties of the field and of the evolution of the atomic system driven by this fluctuating field, we find it very difficult to develop a clear qualitative physical picture for this interaction which adequately describes the asymmetry of these peaks between positive and negative delay times. Our standard picture of the Bloch vector precessing about the electric-field vector is obscured by the fact that only part of the dipole moment is phase matched to radiate into the phase-conjugate beam. The evolution of this component of the dipole moment, which we label $\sigma_{21}^{(-1)}$, does not follow such a simple model. We can gain some insight into this interaction, however, using our numerical methods (described in the Appendix) to determine the magnitude of the phase-conjugate four-wave-mixing signal when the system is driven by a cw laser field which undergoes a single-phase jump of magnitude $\Delta\phi$. We concentrate our efforts on the time evolution of the real and imaginary amplitudes of $\sigma_{21}^{(-1)}$. We allow the probe beam to be delayed with respect to the pump beam by τ_d, consistent with the experiments and calculations described above for the phase diffusion field. With the laser field turned on and the phase at its initial value, the Bloch vector quickly reaches a steady-state condition, producing a phase-conjugate beam of constant amplitude. As the phases of the incoming pump and probe field jump, however, the Bloch vector must converge on a new equilibrium value, with the phase of the new

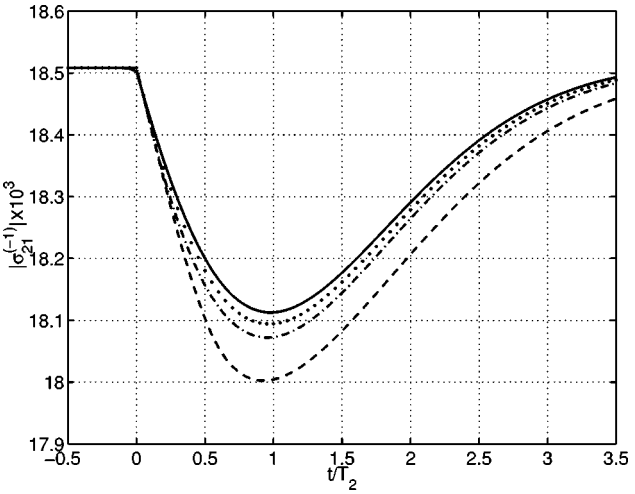

FIG. 7. The magnitude of the phase-matched dipole moment vs time for a laser field undergoing a single-phase jump of magnitude $\Delta\phi = \pi/10$. The four curves correspond to delay times of $\tau_d = -T_2/10$ (solid line), 0 (dotted line), $+T_2/10$ (dot-dashed line), and $+T_2/2$ (dashed line).

dipole moment term also shifting by precisely $\Delta\phi$. In regions of the standing wave pattern where the local Rabi frequency is large $[2\Omega\cos(\vec{k}_f\cdot\vec{r}) > T_2^{-1}]$, the dipole undergoes damped rapid oscillation, and the trajectory of the complex dipole moment depends sensitively on the delay between the pump and probe beams. Even a difference in delay time of $T_2/10$ produces a radically different response. From the respect of attempting to understand the phase-conjugate signal as a function of delay, then, it is fortunate that the phase-conjugate signal is dominated by the contributions where the local Rabi frequency is small $[2\Omega\cos(\vec{k}_f\cdot\vec{r}) \simeq T_2^{-1}]$, where the trajectories are, by comparison, very simple. At these intensities, we observe that the initial response of the dipole moment, $|\sigma_{21}^{(-1)}|$, is always toward smaller magnitudes. This is illustrated in Fig. 7, where we show the calculated magnitude $|\sigma_{21}^{(-1)}|$ as a function of time for four different values of τ_d. The local Rabi frequency for these curves is $0.97T_2^{-1}$. After the initial decrease, the dipole moment rises back to the equilibrium value on a time scale of several T_2. There is no rapid oscillation of the dipole term at these locations since the Rabi frequency and the decay rate are of approximately the same magnitude. We calculate that the decrease in the dipole moment is greatest when the probe beam is delayed by $\tau_d \simeq T_2/2$ (the dashed line in Fig. 7), or longer with respect to the pump beam. Similarly, the decrease in the magnitude of the dipole moment is the smallest for slightly negative delays. In Fig. 7 the solid line corresponds to a delay time of $\tau_d = -T_2/10$. This behavior is similar to what we observe in the phase-conjugate signal for the phase-diffusing laser field. With the phase-diffusing field, or course, the dipole term is constantly out of equilibrium with the laser field, as the phase shifts for this field are random and continuous. Nonetheless, the tendency for phase jumps of the optical phase to suppress the magnitude of the dipole might still reasonably carry over to the phase-diffusing field, lending some level of understanding to this observation.

The peak FWM intensity is only a weak function of the laser bandwidth, b, at high intensities. In this case the rapid

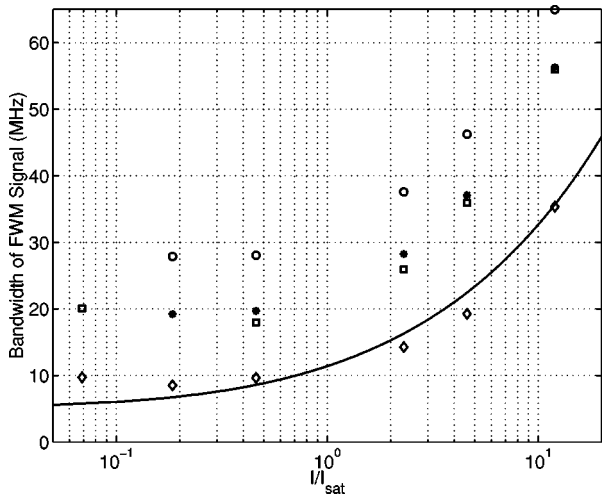

FIG. 8. Bandwidth (FWHM) of the FWM spectrum vs the intensity of the pump laser. Data are shown for laser bandwidths of 24 MHz (○), 14 MHz (*), and 9 MHz (□), and with the external noise off (◇). The solid line is the result of the theory of Abrams and Lind [32] for monochromatic laser fields, as given in Eq. (A9).

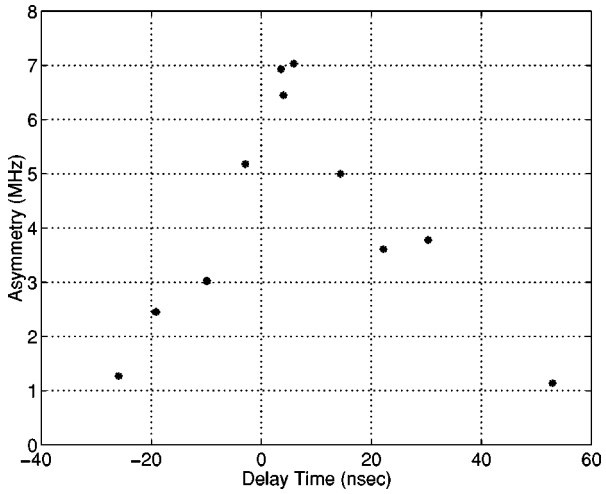

FIG. 9. Asymmetry of the FWM spectrum vs the delay time τ_d. The spectral width of the pump and probe fields is 24 MHz, and the pump-beam intensity is $I/I^0_{\rm sat}=4.6$ ($\Omega/2\pi=15$ MHz).

oscillation of the system at the Rabi frequency dominates, $\Omega \gg b, \Gamma_0, \gamma_{12}$, and the normalized FWM signal for small τ_d approaches unity, i.e., the fluctuations of the laser affect the signal strength only minimally.

We consider the experimental data shown for the highest pump intensity and the lowest pump intensity to be the least reliable because of the smaller signal size and, in the former case, the instability of the signal. There is some discrepancy between the normalized FWM signal strength for theory and experiment for large delay times, as seen for example in Fig. 4(a). Since the experimental values of the normalized FWM signal appear to approach the same value for large negative and large positive values of τ_d, we have confidence in their reliability. Possible causes for the disagreement include (1) the 2-nsec delay between the forward and backward pump beams in the experiment, (2) the finite bandwidth ($\sim$250 kHz) of the narrow-band laser field, (3) the effect of the transverse velocity distribution of the atomic beam, and (4) small deviations between the synthesized laser spectrum and that of the phase diffusion model. None of these factors are included in the numerical simulations. We have previously observed that the third of these plays an important role in the FWM signal strength for narrow-band fields [28], but it is not clear to us how the Doppler broadening effects may be different for narrow-band and broadband excitation.

Our experimental measurements show that the bandwidth of the FWM signal is relatively independent of the delay time between the pump and probe fields. However, the bandwidth of the FWM spectrum is a strong function of the laser bandwidth and the laser intensity. In Fig. 8, we show the mean of the FWM signal bandwidth as a function of laser intensity. Data are shown in this figure for laser bandwidths of 24 MHz (○), 14 MHz (*), and 9 MHz (□), and with the external noise off (◇). The solid line in this figure is the result of the theory of Abrams and Lind [31], as given in Eq. (A9), valid for excitation by a narrow-band laser field. Over the range of our measurements, the bandwidth of the FWM spectrum is a few MHz larger for the 14-MHz laser than for the 9-MHz laser. The bandwidth of the spectra for the 24-MHz laser is larger than that for the monochromatic laser by $\sim$20 MHz.

Although the widths of the spectra do not vary significantly with delay, we do observe a strong dependence of the *shape* of the FWM spectra on the delay time. For large laser intensity, large laser bandwidth, and small positive delay, the FWM spectra become very asymmetric. The peak FWM intensity still occurs near $\Delta=0$, where $\Delta=\omega_L-\omega_{21}$ is the detuning of the laser frequency from the resonance frequency of the atomic transition, ω_{21}. The signal strength for $\Delta>0$ is enhanced, while for $\Delta<0$ it is depleted. In Fig. 9 we show the peak asymmetry as a function of τ_d for $b/\pi=24$ MHz and $I/I^0_{\rm sat}=4.6$. We define the asymmetry of the peak as $(\Delta_+ + \Delta_-)/2$, where Δ_+ (Δ_-) is the detuning of the laser on the high- (low-) frequency side of the peak at which the FWM signal strength is decreased to one-half its peak value. We did not compute any FWM spectra for comparison with the experimental data shown in Figs. 8 and 9, because of the excessive computation time required for this calculation which would provide results of only secondary interest. We consider the peak FWM signal to be of primary interest, and therefore concentrated our computational efforts in that direction.

IV. CONCLUSIONS

In this work we have explored the role of the partial coherence of the laser field on phase-conjugate four-wave mixing. By use of time-delayed pump and probe fields which we derive from the same source, the field statistics become non-Markovian, and complex correlations between the field components which drive the system become very important. In the limit of a large pump intensity and short delays, the evolution of the system at the Rabi frequency dominates the behavior, and the signal is relatively unaffected by the fluctuations of the frequency and phase of the laser. As the delay time increases, however, the FWM signal rapidly decreases due to opposing effects on the system evolution by the pump and probe fields. For low intensities, we understand our observations in terms of the spectral overlap of the laser spec-

trum and the natural linewidth of the atomic sodium used for the measurements. While the computational and experimental results are in reasonable agreement, we hope that these experiments will stimulate the development of analytical techniques and other theoretical efforts into the coherent interaction of quantum systems with non-Markovian fields.

ACKNOWLEDGMENTS

We are grateful for contributions by M. H. Anderson and Ce Chen to the initiation of this project. Gautum Vemuri has graciously given us the numerical code for computing the time-dependent phase diffusion model field. This material was based upon work supported by the U.S. Army Research Office under Grant No. DAAH04-95-1-0361. We also acknowledge the support of the NSF in the early stages of the work carried out at JILA.

APPENDIX: THEORY

In this appendix, we discuss our numerical analysis of the nonlinear interaction of a two-level quantum system with a phase-diffusing laser field which leads to the phase-conjugate four-wave mixing signal. The goal of this analysis is to determine the peak PCFWM intensity for comparison with our experimental results. We integrate the optical Bloch equations for this system to determine the time evolution of the density matrix of the system. We evaluate these elements for an arbitrary field strength of the pump laser, but we restrict the probe laser field to values much less than that required to saturate the transition. Our approach allows us to easily identify the terms which are properly phase matched to radiate in the direction of the signal beam. This analysis has much in common with that presented in Ref. [28], in which we considered the effect of Doppler broadening on PCFWM with monochromatic fields.

The net field incident upon the atomic medium is given by

$$\begin{aligned}\vec{\mathcal{E}}(\vec{r},t)=\hat{\epsilon}\{&E_f\cos(\vec{k}_f\cdot\vec{r}-\omega_L t-\phi(t))\\&+E_b\cos(-\vec{k}_f\cdot\vec{r}-\omega_L t-\phi(t))\\&+E_p\cos(\vec{k}_p\cdot\vec{r}-\omega_L(t-\tau_d)-\phi(t-\tau_d))\}.\end{aligned}\tag{A1}$$

$$=\frac{1}{2}\{\vec{E}(\vec{r},t)e^{-i\omega_L t}+\vec{E}^*(\vec{r},t)e^{i\omega_L t}\},\tag{A2}$$

where

$$\begin{aligned}\vec{E}(\vec{r},t)=\hat{\epsilon}\{&E_f e^{i\vec{k}_f\cdot\vec{r}-i\phi(t)}+E_b e^{-i\vec{k}_f\cdot\vec{r}-i\phi(t)}\\&+E_p e^{i\vec{k}_p\cdot\vec{r}+i\omega_L\tau_d-i\phi(t-\tau_d)}\}.\end{aligned}\tag{A3}$$

The field amplitudes of the forward pump, backward pump, and probe fields are given by E_f, E_b, and E_p, respectively. We use $\vec{k}_b=-\vec{k}_f$ in Eq. (A1) to represent counterpropagation of the forward and backward pump beams. All three beams are degenerate at a frequency ω_L, and the delay time between the pump beam and the probe beam is given by τ_d. The polarization of the laser field is $\hat{\epsilon}$, and $\vec{E}^*(\vec{r},t)$ is the complex conjugate of the field amplitude $\vec{E}(\vec{r},t)$. The forward and backward pump beams form a standing-wave pattern in the medium, and are of nearly the same amplitude ($E_b\simeq 0.98E_f$). We let $E_b=E_f$ in our analysis, and we do not include the effect of the 2-nsec delay between the forward and backward pump beams.

The temporal evolution of the quantum state of the atomic system is described by the equations of motion of the density matrix,

$$\begin{aligned}\dot{\rho}_{21}&=-i\omega_{21}\rho_{21}-\frac{i}{\hbar}V_{21}(\rho_{11}-\rho_{22})-\frac{\rho_{21}}{T_2},\\\dot{\rho}_{11}&=-\frac{i}{\hbar}\{V_{12}\rho_{21}-V_{21}\rho_{12}\}+\frac{\rho_{22}}{T_1},\\\dot{\rho}_{22}&=-\dot{\rho}_{11},\end{aligned}\tag{A4}$$

where the diagonal elements of the density matrix represent the probability of occupation of the excited and ground atomic levels (of energy $\hbar\omega_2$ and $\hbar\omega_1$, respectively), and the off-diagonal elements include the complex oscillatory dipole moment, i.e. the coherence, of the system. The term $\hbar\omega_{21}\equiv\hbar(\omega_2-\omega_1)$ represents the energy difference between the atomic states. The components of the interaction energy matrix are $V_{ij}=-\vec{\mu}_{ij}\cdot\vec{\mathcal{E}}(\vec{r},t)$, where $\vec{\mu}=e\vec{r}$ is the transition electric dipole moment. The elements of the density matrix are a strong function of position because of the standing-wave pattern created by the counterpropagating pump beams. The decay of the population of the upper state has a lifetime $T_1=\Gamma_0^{-1}$, while the coherence has a lifetime $T_2=\gamma_{12}^{-1}$. Moving into a rotating frame through the substitution $\rho_{21}=\sigma_{21}e^{-i\omega_L t}$ and $\rho_{ii}=\sigma_{ii}$ and keeping only the terms which evolve at frequencies much less than optical frequencies, allows one to write

$$\begin{aligned}\dot{\sigma}_{21}&=\left(i\Delta-\frac{1}{T_2}\right)\sigma_{21}-\frac{i}{2\hbar}\vec{\mu}_{21}\cdot\vec{E}(\vec{r},t)W,\\\dot{W}&=\frac{-W-1}{T_1}+\frac{i}{\hbar}\{\vec{\mu}_{21}\cdot\vec{E}(\vec{r},t)\sigma_{12}-\vec{\mu}_{12}\cdot\vec{E}^*(\vec{r},t)\sigma_{21}\}.\end{aligned}\tag{A5}$$

The population probability difference is given by $W=\rho_{22}-\rho_{11}$, and since the atomic system is effectively closed (i.e., the atoms must be in one state or the other), we use $\rho_{11}+\rho_{22}=1$. The detuning of the optical frequency ω_L from the resonant transition frequency ω_{21} is given by $\Delta=\omega_L-\omega_{21}$. We next expand the dipole moment $\sigma_{21}(\vec{r},t)$ and the population difference $W(\vec{r},t)$ in a power series of the factor $e^{i\vec{k}_p\cdot\vec{r}}$ from the probe field,

$$\begin{aligned}\sigma_{21}(\vec{r},t)&=\sigma_{21}^{(0)}(\vec{r},t)+\sigma_{21}^{(1)}(\vec{r},t)e^{i\vec{k}_p\cdot\vec{r}}+\sigma_{21}^{(-1)}(\vec{r},t)e^{-i\vec{k}_p\cdot\vec{r}},\\W(\vec{r},t)&=W^{(0)}(\vec{r},t)+W^{(1)}(\vec{r},t)e^{i\vec{k}_p\cdot\vec{r}}+W^{(-1)}(\vec{r},t)e^{-i\vec{k}_p\cdot\vec{r}}.\end{aligned}\tag{A6}$$

When we gather terms from these equations according to common powers of $e^{i\vec{k}_p\cdot\vec{r}}$, we arrive at a set of six coupled equations,

$$\left(\frac{d}{dt}+\frac{1}{T_2}-i\Delta\right)\sigma_{21}^{(0)}(\vec{r},t)=-i[\Omega(t)\cos(\vec{k}_f\cdot\vec{r})W^{(0)}(\vec{r},t)+\Omega_p(t-\tau_d)W^{(-1)}(\vec{r},t)/2],$$

$$\left(\frac{d}{dt}+\frac{1}{T_2}-i\Delta\right)\sigma_{21}^{(1)}(\vec{r},t)=-i[\Omega(t)\cos(\vec{k}_f\cdot\vec{r})W^{(1)}(\vec{r},t)+\Omega_p(t-\tau_d)W^{(0)}(\vec{r},t)/2],$$

$$\left(\frac{d}{dt}+\frac{1}{T_2}-i\Delta\right)\sigma_{21}^{(-1)}(\vec{r},t)=-i\Omega(t)\cos(\vec{k}_f\cdot\vec{r})W^{(-1)}(\vec{r},t),$$

$$\left(\frac{d}{dt}+\frac{1}{T_1}\right)W^{(0)}(\vec{r},t)=i[(2\Omega(t)\cos(\vec{k}_f\cdot\vec{r})\sigma_{21}^{(0)*}(\vec{r},t)+\Omega_p(t-\tau_d)\sigma_{21}^{(1)*}(\vec{r},t))$$
$$-(2\Omega^*(t)\cos(\vec{k}_f\cdot\vec{r})\sigma_{21}^{(0)}(\vec{r},t)+\Omega_p^*(t-\tau_d)\sigma_{21}^{(1)}(\vec{r},t))]-\frac{1}{T_1}, \tag{A7}$$

$$\left(\frac{d}{dt}+\frac{1}{T_1}\right)W^{(1)}(\vec{r},t)=i[(2\Omega(t)\cos(\vec{k}_f\cdot\vec{r})\sigma_{21}^{(-1)*}(\vec{r},t)+\Omega_p(t-\tau_d)\sigma_{21}^{(0)*}(\vec{r},t))-2\Omega^*(t)\cos(\vec{k}_f\cdot\vec{r})\sigma_{21}^{(1)}(\vec{r},t)],$$

$$\left(\frac{d}{dt}+\frac{1}{T_1}\right)W^{(-1)}(\vec{r},t)=i[2\Omega(t)\cos(\vec{k}_f\cdot\vec{r})\sigma_{21}^{(1)*}(\vec{r},t)-(2\Omega^*(t)\cos(\vec{k}_f\cdot\vec{r})\sigma_{21}^{(-1)}(\vec{r},t)+\Omega_p^*(t-\tau_d)\sigma_{21}^{(0)}(\vec{r},t))].$$

The $\sigma_{21}^{(-1)}(\vec{r},t)$ term represents the amplitude of the dipole moment which radiates the phase-conjugate beam, as indicated by Eq. (A6). $\Omega(t)=\vec{\mu}_{21}\cdot\hat{\epsilon}E_f e^{-i\phi(t)}/\hbar$ is the Rabi frequency of the Bloch vector due to the interaction of an atom with one pump beam, and $\Omega_p(t-\tau_d)=\vec{\mu}_{21}\cdot\hat{\epsilon}E_p e^{-i\phi(t-\tau_d)}/\hbar$ is the Rabi frequency due to the interaction with the probe beam.

We simulate the phase diffusion laser field in our analysis using an algorithm developed by Fox *et al.* [32]. Their procedure uses a random number generator to produce a sequence of values for the laser frequency. We have evaluated the correlation function of the laser frequency and of the laser field, and find them to be in good agreement with the expected correlation functions.

Our analysis of the intensity of the four-wave mixing signal is carried out by numerically integrating Eqs. (A7). We let the transverse relaxation time T_2 be equal to twice the population decay time T_1, consistent with the collision-free trajectories of the atomic sodium beam. We choose the time increment in the integration to be $T_2/1000$. Initial conditions for the Bloch vector are $\sigma_{21}(0)=0$ and $W(0)=-1$, i.e., all the population is in the lower state, and the dipole moment is zero. We turn on the field and let the atomic system evolve for $3T_2$ in order to reach equilibrium with the fluctuating optical field. The pump field creates a standing-wave pattern in the medium, so the evolution of the atomic system depends upon its location within the field. The FWM signal intensity is proportional to the square of the sum of $\sigma_{21}^{(-1)}$, where the summation extends over the length of the interaction region. Since the field pattern is periodic, we carry out the temporal integration at 41 different locations within the standing-wave pattern, spaced by $\lambda/80$ and extending from one antinode of the field to the adjacent antinode, and sum these dipole moments. The transverse intensity profile of pump beam is not a factor in these calculations, since in the experiment we use a probe beam whose diameter is small compared to that of the pump. Within the dimensions of the probe beam, the intensity variations of the pump beam are small.

In order to determine the FWM signal intensity and its uncertainty, we compute the average signal for each $3T_2$ time interval. This integration time is long enough that the average signal within one interval is statistically uncorrelated with the average signal over the previous or following interval. We compute the mean and the standard deviation of the mean using the values produced over the successive individual $3T_2$ intervals. The numerical integration continues until the relative uncertainty of the FWM intensity decreases below a value of 1% of the FWM intensity in the absence of noise, or until the interval of integration reaches $600T_2$, whichever comes first.

One check on the validity of the expansion in Eqs. (A6) and of this computational technique is to determine the amplitude and bandwidth of the FWM signal under conditions of excitation by a monochromatic source, i.e., with the laser frequency and phase noise turned off. We can then use the results of Abrams and Lind [32] for a direct quantitative comparison. We showed these results in Ref. [28]. In the limit of a small (field amplitude) absorption coefficient α_0 in the medium of length L, and with the forward and backward pump beams of equal intensity, one can show that the Abrams and Lind theory yields

$$I_{\mathrm{FWM}}(\Delta=0)=(\alpha_0 L)^2\frac{(2I/I_{\mathrm{sat}}^0)^2}{(1+2I/I_{\mathrm{sat}}^0)^3}I_p \tag{A8}$$

and

$$\Delta\omega_{\mathrm{FWHM}}=\frac{2}{T_2}\sqrt{(\sqrt[3]{2}-1)(1+4I/I^0_{\mathrm{sat}})}, \qquad \text{(A9)}$$

for the intensity I_{FWM} and spectral width $\Delta\omega_{\mathrm{FWHM}}$ of the phase-conjugate signal. Our numerical results are in excellent agreement with the analytic expressions of Eqs. (A8) and (A9). We start to see some anomolies in our results as the pump intensity approaches 60 I^0_{sat}, but this value is well in excess of the intensities we can achieve in our experiments.

Using this technique, we have calculated the peak, i.e., $\Delta=0$ FWM intensity, as a function of the delay time, τ_d. We normalized these intensities by dividing by the FWM intensity calculated for monochromatic fields. The results of these computations are shown in Figs. 4, 5, and 6. We did not compute any FWM spectra using this technique. The numerical computations we have described require a great deal of computer time, and we consider the peak FWM signal to be of greater interest than the spectra. Should FWM spectra be of interest, they could, of course, be determined by numerical integration of Eq. (A7) for varying values of Δ.

[1] R. Beach and S. R. Hartmann, Phys. Rev. Lett. **53**, 663 (1984); R. Beach, D. DeBeer, and S.R. Hartmann, Phys. Rev. A **32**, 3467 (1985).

[2] S. Asaka, H. Nakatsuka, M. Fujiwara, and M. Matsuoka, Phys. Rev. A **29**, 2286 (1984); H. Nakatsuka, M. Tomita, M. Fujiwara, and S. Asaka, Opt. Commun. **52**, 150 (1984).

[3] Norio Morita and Tatsuo Yajima, Phys. Rev. A **30**, 2525 (1984).

[4] P. Ye and Y. R. Shen, Phys. Rev. A **25**, 2183 (1982).

[5] M. Fujiwara, R. Kuroda, and H. Nakatsuka, J. Opt. Soc. Am. B **2**, 1634 (1985).

[6] J. E. Golub and T. W. Mossberg, J. Opt. Soc. Am. B **3**, 554 (1986); Opt. Lett. **11**, 431 (1986).

[7] N. Morita, K. Torizuka, and T. Yajima, J. Opt. Soc. Am. B **3**, 548 (1986).

[8] M. Tomita and M. Matsuoka, J. Opt. Soc. Am. B **3**, 560 (1986).

[9] T. Hattori, A. Terasaki, and T. Kobayashi, Phys. Rev. A **35**, 715 (1987).

[10] K. Kurokawa, T. Hattori, and T. Kobayashi, Phys. Rev. A **36**, 1298 (1987).

[11] G. L. Huang and H. S. Kwok, J. Opt. Soc. Am. B **9**, 2019 (1992).

[12] M. Defour, J.-C. Keller, and J.-L. Le Gouët, J. Opt. Soc. Am. B **3**, 544 (1986).

[13] M. Defour, J.-C. Keller, and J.-L. Le Gouët, Phys. Rev. A **36**, 5226 (1987).

[14] P. Tchénio, A. Débarre, J.-C. Keller, and J.-L. Le Gouët, J. Opt. Soc. Am. B **5**, 1293 (1988); Phys. Rev. A **39**, 1970 (1989).

[15] P. Tchénio, A. Débarre, J.-C. Keller, and J.-L. Le Gouët, Phys. Rev. A **38**, 5235 (1988).

[16] P. Tchénio, A. Débarre, J.-C. Keller, and J.-L. Le Gouët, Phys. Rev. Lett. **62**, 415 (1989).

[17] R. Friedberg and S. R. Hartmann, J. Phys. B **21**, 683 (1988).

[18] V. Finkelstein and P. R. Berman, Phys. Rev. A **41**, 6193 (1990).

[19] V. Finkelstein and P. R. Berman, Phys. Rev. A **42**, 3145 (1990).

[20] G. Vemuri, G. S. Agarwal, R. Roy, M. H. Anderson, J. Cooper, and S. J. Smith, Phys. Rev. A **44**, 6009 (1991).

[21] G. Vemuri, Phys. Rev. A **48**, 3256 (1993).

[22] P. Ewart and P. Snowdon, Opt. Lett. **15**, 1403 (1990).

[23] D. R. Meacher, A. Charlton, P. Ewart, J. Cooper, and G. Alber, Phys. Rev. A **42**, 3018 (1990).

[24] P. G. R. Smith and P. Ewart, Phys. Rev. A **54**, 2347 (1996).

[25] R. Bratfalean and P. Ewart, Phys. Rev. A **56**, 2267 (1997).

[26] K. Gheri, M. A. M. Marte, and P. Zoller, J. Opt. Soc. Am. B **8**, 1559 (1991).

[27] M.H. Anderson, G. Vemuri, J. Cooper, P. Zoller, and S. J. Smith, Phys. Rev. A **47**, 3202 (1993).

[28] Binh Do, J. W. Cha, D. S. Elliott, and S. J. Smith, Phys. Rev. A **58**, 3089 (1998).

[29] D. S. Elliott and S. J. Smith, J. Opt. Soc. Am. B **5**, 1927 (1988).

[30] R. E. Grove, F. Y. Wu, and S. Ezekial, Phys. Rev. A **15**, 227 (1977).

[31] R. L. Abrams and R. C. Lind, Opt. Lett. **2**, 94 (1978); **3**, 205 (1978); R. L. Abrams, J. F. Lam, R. C. Lind, D. G. Steel, and P. F. Liao, in *Optical Phase Conjugation*, edited by Robert A. Fisher (Academic, San Diego, 1983), Chap. 8.

[32] R. F. Fox, I. R. Gatland, R. Roy, and G. Vemuri, Phys. Rev. A **38**, 5938 (1988).